THE ASTROPHYSICAL JOURNAL, 473:L71–L74, 1996 December 20
© 1996. The American Astronomical Society. All rights reserved. Printed in U.S.A.

DETECTION OF A TEMPERATURE STRUCTURE IN THE COMA CLUSTER OF GALAXIES WITH *ASCA*

H. HONDA,[1,2] M. HIRAYAMA,[1,3] M. WATANABE,[4] H. KUNIEDA,[4] Y. TAWARA,[4] K. YAMASHITA,[4]
T. OHASHI,[5] J. P. HUGHES,[6] AND J. P. HENRY[7]
Received 1996 July 8; accepted 1996 October 4

ABSTRACT

Significant temperature variation is found from *ASCA* observations of the hot intracluster medium in the Coma cluster of galaxies. The whole cluster out to 1° from the center was covered by 14 pointings. The temperature of the hot gas in the outside region is estimated by correcting for the stray-light effect from the bright center. The inferred temperature is lower than 4.5 keV in the west region and higher than 10 keV in the east, both offset by 40′ (1.6 Mpc for $H_0 = 50$ km s^{-1} Mpc^{-1}) from the center. The temperature variation is not explained by a systematic error in the complex point-spread function of the *ASCA* X-ray telescope. The azimuthal variation of temperature is probably caused by recent mergers and may reflect an extended distribution of the dark matter.

Subject headings: galaxies: clusters: individual (Coma) — galaxies: intergalactic medium — X-rays: galaxies

1. INTRODUCTION

The Coma Cluster had been recognized as an archetype of rich and relaxed clusters until recent *ROSAT* observations revealed that the intracluster medium (ICM) has a complex distribution (Briel, Henry, & Böhringer 1992; White, Briel, & Henry 1993). The X-ray surface brightness distribution shows a secondary peak around the galaxy NGC 4839, at 40′ southwest from the cluster's center, and it corresponds to the substructure seen in the projected galaxy distribution map (Mellier et al. 1988). Merger scenarios have been proposed to account for the X-ray features in the Coma Cluster (e.g., Burns et al. 1994). The slow mass-flow rate and the cooling time, longer than the Hubble time, in the Coma Cluster (Edge, Stewart, & Fabian 1992) suggest the absence of cooling flows in the central region. The relatively high temperature, ~8 keV, has prevented accurate measurement of the temperature distribution with *ROSAT*.

Works by Hughes and others (Hughes, Gorenstein, & Fabricant 1988a; Hughes et al. 1988b; Hughes 1989; Watt et al. 1992) show that the core of the cluster is nearly isothermal out to a radius of 1° and suggest that the temperature falls with radius beyond that. Hughes et al. (1993), based on a recent analysis of the *Ginga* scanning observations, showed that the ICM is approximately isothermal in the core and becomes cooler beyond several core radii. In this Letter, we present a significant detection of a temperature distribution of the ICM in the Coma Cluster over a radius of 1° observed with *ASCA*.

[1] Institute of Space and Astronautical Science, 1-1 Yoshinodai, 3-chome, Sagamihara, Kanagawa 229, Japan.
[2] Department of Physics, Tokai University, 1117 Kitakaname, Hiratsuka, Kanagawa 259-12, Japan.
[3] Department of Physics, University of Tokyo, 7-3-1 Hongo, Bunkyo-ku, Tokyo 113, Japan.
[4] Department of Physics, Nagoya University, Chikusa-ku, Nagoya 464-01, Japan.
[5] Department of Physics, Tokyo Metropolitan University, Hachioji, Tokyo 192-03, Japan.
[6] Harvard-Smithsonian Center for Astrophysics, 60 Garden Street, Cambridge, MA 02138.
[7] Institute for Astronomy, University of Hawaii, 2680 Woodlawn Drive, Honolulu, HI 96822.

2. OBSERVATIONS

The spectroscopic imaging observation of the Coma Cluster was carried out with the *ASCA* satellite (Tanaka, Inoue, & Holt 1994), using 14 pointings to cover the angular region within 60′ from the center. The observed region extends well beyond that within which isothermality has been established. The net exposure and field of view of each observation were about 10 ks and 20′ in radius, respectively. The first six observations were performed on 1993 June 14–16, during the PV phase. *ASCA* pointed the central region of the Coma Cluster (hereafter POS0), four regions ~20′ away from the X-ray center (POS1–POS4), and a region including the subcluster (POS5). The rest of the observations were carried out on 1994 June 6–11 as *ASCA* AO-2 observations. Regions ~40′ away from the center of the cluster were observed in this period (POS6–POS13). All pointing positions are displayed in Figure 1 (Plate L11).

3. ANALYSIS AND RESULTS

A contour map of the X-ray surface brightness in the 0.7–10 keV energy range, obtained with *ASCA*'s gas imaging spectrometer (GIS), is shown in Figure 1, which is essentially consistent with the *ROSAT* results in the soft X-ray band (White et al. 1993). For the image and following analysis in this Letter, only the data from the GIS instrument (Ohashi et al. 1996; Makishima et al. 1996) are used. We first selected photons with standard criteria, i.e., photons detected in time zones with cosmic-ray cutoff rigidity greater than 8 GeV c^{-1} and elevation from Earth of a pointing direction greater than 5°.

For each observation, photons within a fixed sky region with a radius of 15′ are accumulated into one GIS spectrum with the GIS2 and GIS3 data combined. This avoids difficulty in modeling the X-ray telescope (XRT) response (Serlemitsos et al. 1995) in the outer part of the GIS field of view. For POS9, the point source at R.A. = 195°.38 and decl. = 28°.64 with a 2′.5 radius is excluded from the analysis. The blank-sky data, supplied by the *ASCA* Guest Observer Facility at the Institute of Space and Astronautical Science and NASA Goddard Space Flight Center, are used to create the background spectrum for all of our spectra. The flux of the cosmic X-ray

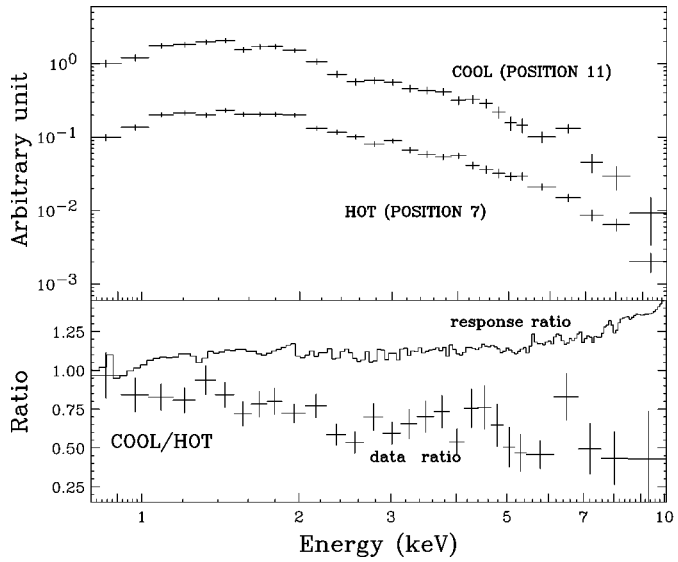

FIG. 2.—Comparison of the X-ray spectra at different positions. *Top*: GIS pulse-height spectra at POS7 and POS11. The two positions are the same distance (40′) from the cluster's center. The vertical scale is arbitrary. *Bottom*: Ratio of the two spectra, compared with the ratio of the response for two regions. Azimuthal dependence of the stray light causes a systematic rise of the response ratio with energy.

background and non–X-ray background can vary by at most 4% rms with the present data selection criteria (Ishisaki 1996). This yields a flux uncertainty of 3% in the regions offset by 40′ from the Coma Cluster's center. The effect on the spectral results is much smaller than that due to the stray light, as discussed below.

Based on the 14 GIS spectra, we looked into the spatial variation of the spectral features. Examples of the raw spectra (corrected only for the non–X-ray and cosmic X-ray background) at different positions, POS7 and POS11, are shown in Figure 2. These positions are offset by 40′ from the cluster's center, and we expect that the effects of stray light on spectral results should be similar, as discussed below. The bottom panel in Figure 2 shows the ratio of the two spectra as a function of energy. For comparison, the ratio of the energy-dependent effective area (indicated as "response ratio" in the figure) for the two regions is also shown. If the two regions have the same temperature, the spectral ratio should follow the response ratio. A significant difference is seen between the spectral ratio and the response ratio, indicating a temperature variation in the Coma Cluster. In order to ensure the result, however, the stray-light properties of the XRT need to be examined in detail.

The observed spectrum at each position is contaminated by the stray light, which consists of photons generated outside of the field of view that pass through the mirror reflected on the back-side surface or with only one reflection. Because of the contamination, it is difficult for *ASCA* to determine individual local temperatures in the cluster when the angular extent of the source exceeds the GIS field of view. The large difference in the surface brightness in the cluster also makes the analysis more difficult; the cluster's center is 20 times brighter than the outermost pointing regions when averaged over a 15′ radius. Table 1 shows the estimated fraction of the flux that originated outside of the pointed region with 15′ radius (the stray light and the tail part in the XRT point-spread function) for different offset positions in the Coma Cluster observations.

TABLE 1

FRACTION OF THE CONTAMINATING LIGHT

Position	Surface Brightness (counts s^{-1})	Stray Light (%)	Tail of XRT Response (%)
Center.....	4.9	3	1
20′ offset.....	1.1	10	8
40′ offset.....	0.26	55	2

The contribution from the stray light is comparable to the normally reflected photons generated within the field of view at 40′ offset from the cluster's center. In this case, ~60% of the stray light comes from the bright central region ($r < 15'$) of the cluster. The true temperature distribution can only be obtained by solving the mutual stray-light contributions to the pulse-height spectra for all the regions in a self-consistent way.

Since it takes some time to work out the fully self-consistent analysis for the whole Coma Cluster, we try here to derive approximate temperatures for the observed regions. This is performed by fitting each observed spectrum, consisting of stray and on-axis photons, to a single-temperature thermal model with a modified response function that partly compensates the stray light's effects. The modification of the response function in principle requires full knowledge about the cluster surface brightness structure and the temperature distribution. For these conditions, we assume here that the ICM is isothermal and follows a β-model with parameters derived from *ROSAT* ($\beta = 0.75$ and $r_{\rm core} = 10.'5$, by Briel et al. 1992), which has a better imaging capability than *ASCA*. This response results in true temperatures for the Coma Cluster only if the ICM is isothermal, and otherwise we obtain approximate ones. Note that, in this approach, no absolute temperatures have to be assumed a priori, since the response function describes only the relative photon contributions between different positions.

Employing these response functions, the 14 observed spectra have been fitted individually with a single-temperature Raymond-Smith model. Free parameters are temperature, metal abundance, and normalization. The neutral hydrogen column density for absorption in the line of sight is fixed at the Galactic value ($N_{\rm H} = 9.1 \times 10^{19}$ cm^{-2}). With 93 degrees of freedom, we obtain reduced χ^2 values of less than 1.2 for all 14 positions. The temperature determined in this way is called the "trial temperature" in this Letter, since it is likely to be different from the true one. The azimuthal distribution of the trial temperatures with a 90% confidence error for a single parameter ($\chi^2_{\rm min} + 2.71$) is shown in Figure 3. The best-fit values range from 5 to 12 keV with significant deviations in their statistical errors. Indeed, even excluding POS11, a hypothesis of constant temperature is rejected with 90% confidence ($\chi^2 = 18.9$ for 12 degrees of freedom), employing conservative systematic errors discussed below. We emphasize that if the temperature were indeed constant all over the Coma Cluster, the response used here would be capable of giving the same and correct value for all positions. Therefore we conclude that the data are inconsistent with the isothermality assumption. In other words, Figure 3 indicates that a large variation of temperature exists in the Coma Cluster. This spectral fit also shows that the metal abundances are 0.1–0.3 times solar, with 90% uncertainties greater than 0.1 times solar in most regions.

Let us briefly consider to what extent we can infer the true temperatures. As shown in Table 1, the central region is

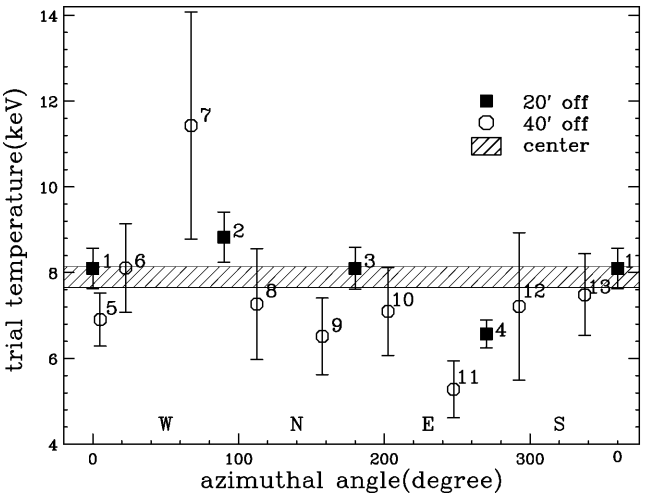

FIG. 3.—"Trial temperatures" (see § 3) obtained for the 14 regions in the Coma Cluster. These are shifted toward 7 keV from the true temperature, and the distribution of the latter should be wider than seen in the figure. The error bars indicate 90% statistical errors. Systematic errors are ~1.5 keV for POS7 and ~0.5 keV for other positions with 40′ offset. The data points appear in order of azimuthal angle with respect to the cluster's center, measured from the direction of NGC 4839 subcluster.

almost free from the stray-light contamination. We estimate that the trial temperature should agree with the true one within 0.2 keV uncertainty, based on model fittings to contaminated spectra simulated assuming various temperatures for other regions. Particularly in the 40′ offset regions, it can be shown that the true range of the temperature variation is wider than that shown in Figure 3. Take a region, for example, where the trial temperature is 10 keV. The temperature results from a mixture of the stray light from the cluster's center and that originating within the field of view. Since the stray light creates a softer pulse-height spectrum than the original 8 keV one by ~1 keV, the true spectrum in the field of view has to be harder than 10 keV in order to counterbalance the contribution from the 7 keV equivalent spectrum due to stray photons. The same effect works in all the regions. The trial temperatures in Figure 3 are, therefore, apparently shifted toward 7 keV from the true values. Taking into account this effect based on the simulations, we found that true temperature is 10 keV or higher at POS7 and 4.5 keV or lower at POS11, with 90% confidence.

Next we estimate the systematic uncertainty in our response function for the XRT. The systematic error in the estimation of the stray-light effect should affect our spectral results. The "ray-tracing" method (Tsusaka et al. 1995) is used to estimate the XRT response in the present analysis. We compare the observed spectra of the Crab Nebula at different offset angles (0′–80′) and those produced by the ray-tracing code (Ishisaki 1996). The simulated spectra agree with the observed ones well: the difference is $\lesssim$30% in the flux and 0.05 in the power-law spectral index. We define uncertainty range of the stray light's intensity (for back-side and single reflection) within which the simulated spectra agree with the observed Crab ones. By changing the stray-light parameters within the uncertainty range, we reproduce the XRT response function and repeat the spectral fit. The change of the best-fit temperatures is 0.5 and 1.5 keV for trial temperatures of 5.3 and 11.4 keV, respectively. We also check systematics due to uncertainties in the β-model parameters assumed. If we change β by 0.03 and $r_{\rm core}$ by 0.′6 (the *ROSAT* error range), the best-fit trial temperature varies by 0.1–0.2 keV in all regions. In conclusion, uncertainties in the ray-tracing code and in the β-model parameters have no effect on the significance of the temperature variation.

It is unlikely that the observed high temperature at POS7 is caused by contamination from a point source such as an active galactic nucleus (AGN). The measured flux corresponds to ~0.5 mcrab (~1×10^{-11} ergs cm^{-2} s^{-1}). To make a significant change in the energy spectrum, the intensity of the contaminating source would have to be on the order of 0.1 mcrab if it were an unobscured AGN spectrum with a photon index of 1.7. Such a point source should be clearly seen in the X-ray image from the GIS or *ROSAT*, which is not the case.

4. DISCUSSION

The significant temperature variation in the Coma Cluster found in the *ASCA* observations presents interesting insights about the cluster's formation. First, the result may imply that the ICM is not under hydrostatic equilibrium, unless the underlying dark matter has a very complex spatial distribution. We know a few clusters that show spatial variations in their temperature. In Abell 2163, a sharp drop of the temperature is detected at ~400 kpc from the center, and it suggests that the electron and ion temperatures are not reaching equilibrium in the outer region of the cluster (Markevitch et al. 1994, 1996). A systematic drop of the temperature in the outer region of the cluster is seen in other systems (Markevitch et al. 1996), but Abell 754 exhibits an asymmetric temperature structure (Henry & Briel 1995; Henriksen & Markevitch 1996). The variation of temperature in the Coma Cluster occurs in a complicated way. It is not a simple drop or rise of kT as a function of radius. POS1–POS4 cover regions 20′ away from the center, but their kT's differ by a factor of 1.5. The difference of temperature with azimuth becomes larger in the outer regions. POS7 and POS11 show kT different by a factor of 2.

Despite the large temperature variation, by a factor of more than 2, the X-ray surface brightness shows no clear corresponding features (see Fig. 1 and White et al. 1993). The hottest region (POS7) shows no point-source features in either *ROSAT* or GIS images, which rules out contamination from AGNs and indicates that the "hot" spectrum is due to the ICM itself. If the cluster had been an isolated system collapsing from self-gravitation, it seems unlikely that the ICM by itself would develop nonaxisymmetric structures. The observed asymmetry in the temperature distribution suggests that external disturbances or interactions have been involved. Recent numerical simulations of the formation of the cluster (e.g., Schindler & Müller 1993) show that, after a subcluster merger, the temperature distribution takes a longer time than the X-ray surface brightness to reach a smooth distribution. The qualitative agreement of this feature with the present result suggests that the Coma Cluster has experienced recent mergers.

The rather complex distribution of the inferred temperature may indicate that several subclusters have been merged to form the present cluster. If a cluster-cluster collision has raised the temperature of the hot region ($\gtrsim$13 keV at POS7) from the average temperature (~8 keV) in the central region, the relative velocity of the collision would be on the order of 1000 km s^{-1}. Such a velocity seems reasonable if the subcluster would acquire it as it fell into the main Coma Cluster

potential. On the other hand, the cool region (POS11) may contain mostly the stripped subcluster gas, which is thought to be relatively cool in the initial state. The numerical simulations (e.g., Schindler & Müller 1993) suggest that the gas would remain unheated for several times 10^9 yr. Recent calculations by Ishizaka & Mineshige (1996) show that even a single subcluster collision with supersonic velocity creates both hot and cool regions in the main cluster. Besides the heating due to direct collision, cooling also occurs in the outer region through adiabatic expansion of the stripped gas.

The locations of the hot (POS7) and cool (POS11) regions are very far from the NGC 4839 subcluster, which may have passed through the Coma Cluster's center in the recent merger event (Burns et al. 1994). The X-ray morphology around NGC 4839 (White et al. 1993) and the recent measurement of galaxy dynamics (Colless & Dunn 1996), however, suggest that NGC 4839 is, rather, approaching the Coma Cluster's center. The absence of strong temperature structure near NGC 4839 suggests that the merger is yet to happen. Also, the present result, in which the heating and cooling occur only in the outskirts, suggests that mergers may be on small scales, in contrast to the simulated features for major mergers (e.g., Roettiger, Burns, & Loken 1993).

The distribution of the dark matter after the subcluster merger is not well understood. According to *N*-body simulations (e.g., Evrard 1990), the dark matter particles pass through during the collision without interactions and take a longer time than the gas to completely merge into a single body. If the Coma Cluster is under an ongoing merger, the dark matter distribution would be very different from and much more extended than the ICM one. The temperature distribution detected here may partly reflect a complex dark matter distribution. This would be contrary to the recent finding that the dark matter distribution in relaxed clusters is more concentrated than the ICM (David, Jones, & Forman 1995). More elaborate study, such as detailed comparison between the data and the simulations, would lead us to a self-consistent view of the distribution of the dark matter, as well as the ICM.

We thank T. Kii and M. Ishida for useful advice and discussion. R. Shibata has supported investigation of the XRT response. Help from the XRT, ASCA_ANL, and SimASCA teams is acknowledged for building the analysis system for extended sources. M. H. received a fellowship from the Japan Society for the Promotion of Science for Junior Scientists.

REFERENCES

Briel, U. G., Henry, J. P., & Böhringer, H. 1992, A&A, 259, L31
Burns, J. O., Roettiger, K., Ledlow, M., & Klypin, A. 1994, ApJ, 427, L87
Colless, M., & Dunn, A. M. 1996, ApJ, 458, 435
David, L. P., Jones, C., & Forman, W. 1995, ApJ, 445, 578
Edge, A. C., Stewart, G. C., & Fabian, A. C. 1992, MNRAS, 258, 177
Evrard, A. E. 1990, in Clusters of Galaxies, ed. W. R. Oegerle, M. J. Fitchett, & L. Danly (Cambridge: Cambridge Univ. Press), 287
Henriksen, M. J., & Markevitch, M. L. 1996, ApJ, 466, L79
Henry, J. P., & Briel, U. G. 1995, ApJ, 443, L9
Hughes, J. P. 1989, ApJ, 337, 21
Hughes, J. P., Butcher, J. A., Stewart, G. C., & Tanaka, Y. 1993, ApJ, 404, 611
Hughes, J. P., Gorenstein, P., & Fabricant, D. 1988a, ApJ, 329, 82
Hughes, J. P., Yamashita, K., Okumura, Y., Tsunemi, H., & Matsuoka, M. 1988b, ApJ, 327, 615
Ishisaki, Y. 1996, Ph.D. thesis, Univ. Tokyo
Ishizaka, C., & Mineshige, S. 1996, PASJ, 48, L37
Makishima, K., et al. 1996, PASJ, 48, 171
Markevitch, M., Mushotzky, R. F., Inoue, H., Yamashita, K., Furuzawa, A., & Tawara, Y. 1996, ApJ, 456, 437
Markevitch, M., Yamashita, K., Furuzawa, A., & Tawara, Y. 1994, ApJ, 436, L71
Mellier, M., Mathez, G., Mazure, A., Chauvineau, B., & Proust, D. 1988, A&A, 199, 67
Ohashi, T., et al. 1996, PASJ, 48, 157
Roettiger, K., Burns, J. O., & Loken, C. 1993, ApJ, 407, L53
Schindler, S., & Müller, E. 1993, A&A, 272, 137
Serlemitsos, P. J., et al. 1995, PASJ, 47, 105
Tanaka, Y., Inoue, H., & Holt, S. S. 1994, PASJ, 46, L37
Tsusaka, Y., et al. 1995, Appl. Opt., 34, 4848
Watt, M. P., Ponman, T. J., Bertram, D., Eyles, C. J., Skinner, G. K., & Willmore, A. P. 1992, MNRAS, 258, 738
White, S. D. M., Briel, U. G., & Henry, J. P. 1993, MNRAS, 261, L8

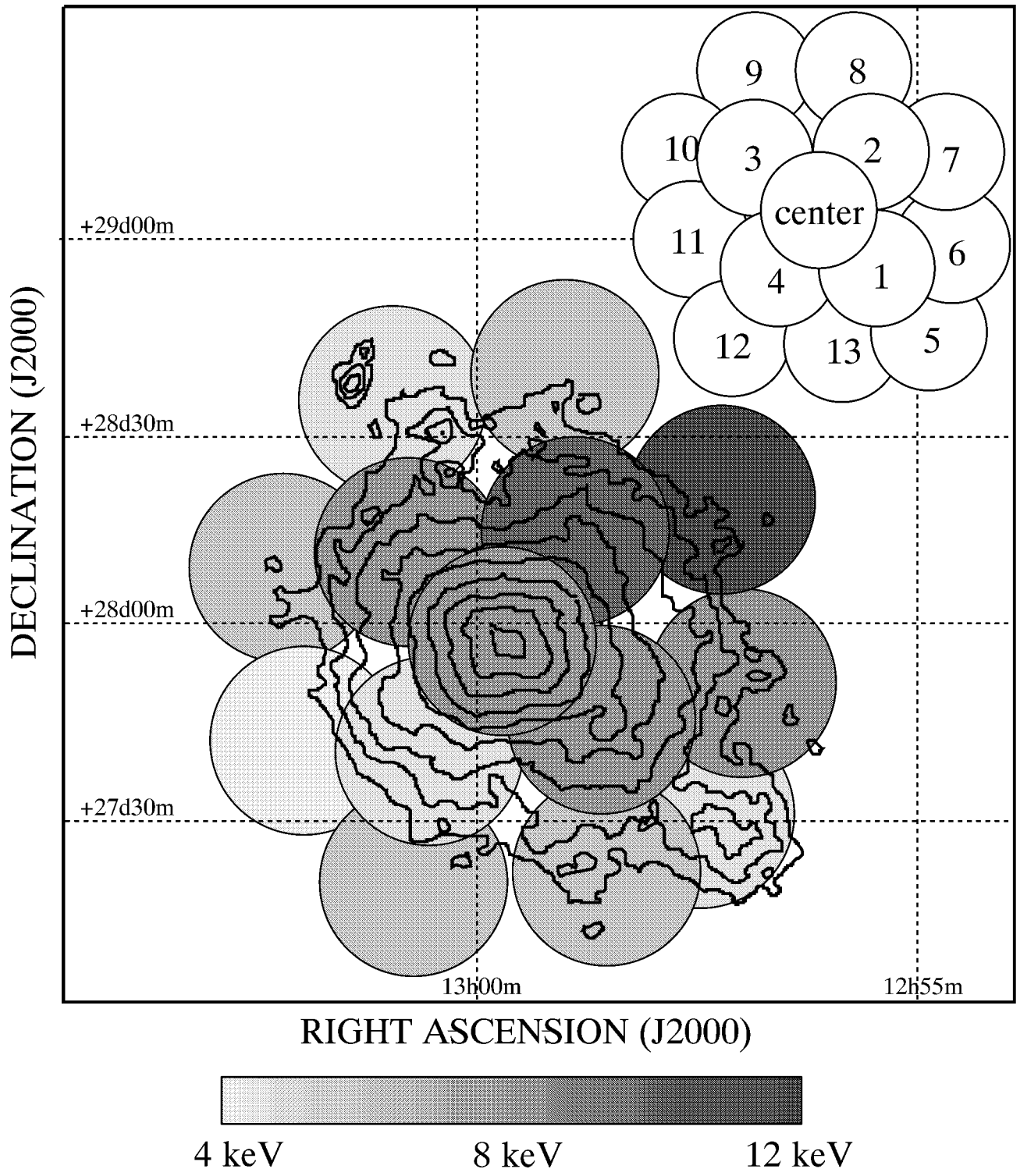

FIG. 1.—Positions of the 14 *ASCA* pointings, displayed with circles tagged with POS0–POS13. The radius of each circle is 15′. The contours of the X-ray surface brightness obtained with the GIS are shown. A gray-scale representation of the "trial temperatures" (see § 3) is also shown.